Supplementary Information
Orbital angular momentum-driven anomalous Hall effect

Oliver Dowinton[1] and Mohammad Saeed Bahramy[1]

[1]*Department of Physics and Astronomy,*
The University of Manchester, Oxford Road,
Manchester M13 9PL, United Kingdom

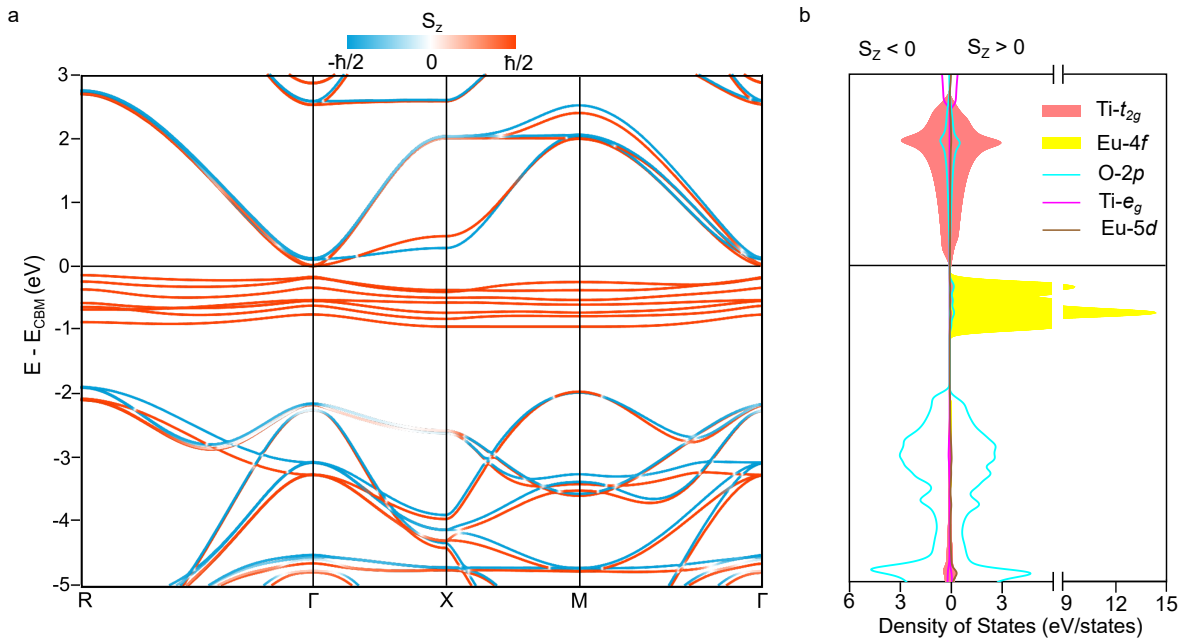

Figure 1. (a) Band-structure of $EuTiO_3$ along the high symmetry points of the Brillouin zone, energy offset against the conduction band minimum (E_{CBM}). (b) Projected density of states in the same energy window.

I. EUTIO3 BAND STRUCTURE

Figure 1 shows a view of the ferromagnetic $EuTiO_3$ band-structure and density of states (DOS) over a larger energy range and through all the high symmetry points of the Brillouin Zone (BZ). We can see that the seven Eu-4f states are entirely spin polarized by the RKKY interaction as expected, and that they form a relatively flat in-gap manifold close to the dispersive Ti t_{2g} states. In the DOS plot we can see the small admixture of O-2p states in the Ti t_{2g} bands, and the lack of any mixing into the Ti e_g or Eu-5d bands.

II. 111 MAGNETIZATION

In this section we'll give more details for the orbital character and OAM texture of the (111) magnetization case, and hence show more explicitly how control over the magnetic field gives control over our system. As discussed in the main text, due to the induced crystal field symmetry, this magnetization direction has considerably less Fermi-surface warping than the (001) case. And, as has already been established, this warping is the result of a varying SO term that arises due to (un)quenched OAM from orbital symmetry properties. Fig 2 shows that the symmetry properties of this magnetization lead to smoother boundaries between regions of orbital character, and importantly that the d_{xy} orbitals are no longer isolated leading to less pronounced OAM quenching. The SAM is still collinear and now directed

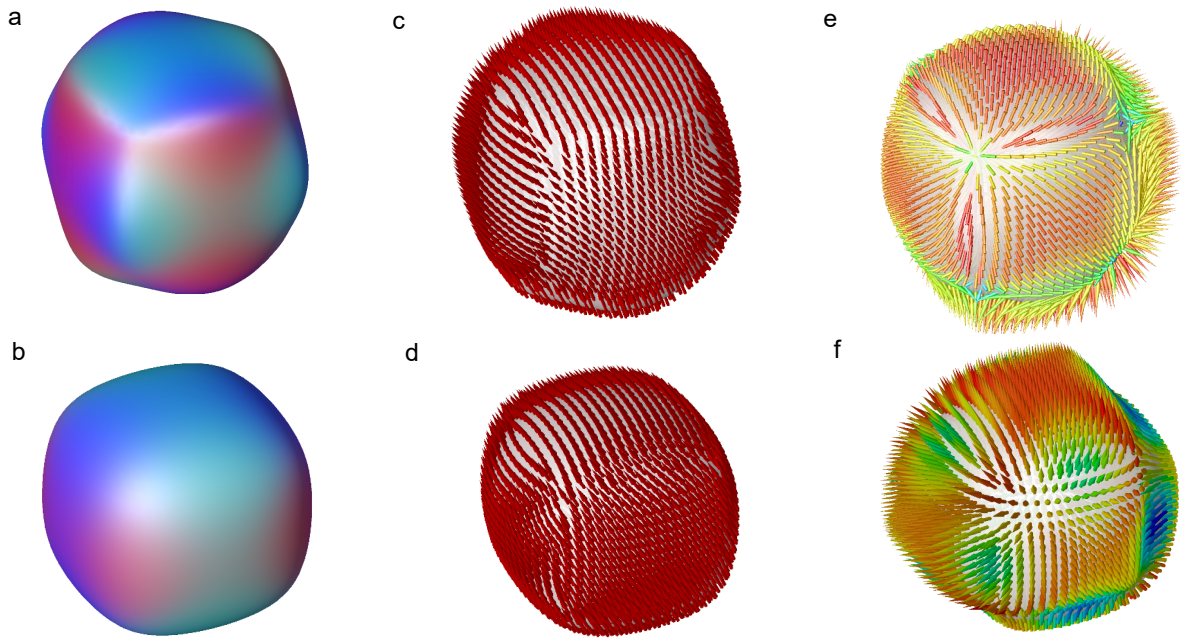

Figure 2. 2nd and 3rd (top and bottom rows respectively) Fermi pockets for (111) magnetization case. (a-b) shows orbital projection, with same colour scheme as the main paper. (c-d) shows SAM. (e-f) shows OAM.

along (111).

III. CRYSTAL FIELD DETAILS

Here we give more explicit mathematical details for how the symmetry of the crsytal field (CF) relates to OAM quenching. Firstly, we show how isolated t_{2g} orbitals lead to quenched OAM. Given that $L_z|Y_l^m\rangle = m|Y_l^m\rangle$, where L_z is the angular momentum operator along z, it is apparent for any state of the form

$$|X\rangle = |Y_l^m\rangle + e^{i\phi}|Y_l^{-m}\rangle, \tag{1}$$

where $\phi \in \mathbb{R}$,

$$\langle X|L_z|X\rangle = 0. \tag{2}$$

In addition, as L_x and L_y only mix $Y_l^m \to Y_l^{m\pm1}$ we can see that

$$\langle X|L_x|X\rangle = \langle X|L_y|X\rangle = 0. \tag{3}$$

Hence, OAM vanishes for any state of the form of $|X\rangle$, which includes the t_{2g} states if we consider their form given in the main paper

$$\begin{aligned} d_{xy} &= \frac{i}{\sqrt{2}}\left(Y_2^2 - Y_2^{-2}\right) \\ d_{xz} &= \frac{1}{\sqrt{2}}\left(Y_2^{-1} - Y_2^1\right) \\ d_{yz} &= \frac{i}{\sqrt{2}}\left(Y_2^{-1} + Y_2^1\right). \end{aligned} \tag{4}$$

Secondly we expand on the 4-fold rotational symmetry of the CF in the x-y plane. The generator of this rotation group is a rotation of $\frac{\pi}{2}$ about the z-axis. Hence to show a CF obeys this symmetry, it is sufficient to show it is invariant under such a $\frac{\pi}{2}$ rotation. If we expand our CF potential in terms of spherical harmonics:

$$V = \sum_{m,n=-l}^{l} V_{m,n}|Y_l^m\rangle\langle Y_l^n|, \tag{5}$$

after rotating we have

$$V \to V' = \sum_{m,n=-l}^{l} V_{m,n}e^{\frac{\pi}{2}(m-n)}|Y_l^m\rangle\langle Y_l^n|. \tag{6}$$

Hence, for V to be invariant under such a rotation we have the requirement that $V_{m,n} \neq 0 \Rightarrow m = n$ or $m - n = \pm 4\alpha$, where α is an integer. As such, the only off-diagonal terms for the t_{2g} states are those that couple the $m = \pm 2$ harmonics. Furthermore from the hermiticity of V and the property that $Y_2^2 = (Y_2^{-2})^*$, we have the results $V_{2,-2} = V_{2,-2}^* = V_{-2,2}^* = V_{-2,2}$ and $V_{2,2} = V_{-2,-,2}$. Hence it is easy to show that the $d_{xy} = \frac{i}{\sqrt{2}}\left(Y_2^{-2} - Y_2^2\right)$ orbital is an eigenstate of the potential, as are the spherical harmonics $Y_2^{\pm 1}$. Consequently, the t_{2g} manifold is further split, with the d_{xy} becoming isolated from the degenerate d_{xz} and d_{yz} orbitals.

IV. BERRY CURVATURE TERM DERIVATION

Here we detail the full derivation of the expression relating OAM texture to the Berry curvature of the Brillouin zone (BZ) as discussed in the main text. For the n^{th} energy eigenstate at $\vec{k}$, $|n(\vec{k})\rangle$, consider the general expression for its contribution to the Berry curvature over a 3D BZ ($\vec{k}$ dependence of $|n\rangle$ is implicit from now on):

$$\vec{\Omega}_n(\vec{k}) = \text{Im}\left[\langle\vec{\nabla}_{\vec{k}}n| \times |\vec{\nabla}_{\vec{k}}n\rangle\right], \tag{7}$$

and use the standard vector algebra identity $(\vec{A}\times\vec{B})\cdot(\vec{C}\times\vec{D}) = (\vec{A}\cdot\vec{C})(\vec{B}\cdot\vec{D}) - (\vec{A}\cdot\vec{D})(\vec{B}\cdot\vec{C})$ to write its magnitude

$$\left|\vec{\Omega}_n(\vec{k})\right|^2 = \sum_{i,j,p,q} \left(\langle\partial_{k_i} n|\partial_{k_j} n\rangle^2 - \langle\partial_{k_p} n|\partial_{k_p} n\rangle\langle\partial_{k_q} n|\partial_{k_q} n\rangle\right). \tag{8}$$

We can then relate this to OAM as follows; First consider that the energy eigenstates must be eigenstates of the spin orbit term $\vec{L}\cdot\vec{S}$, and given that at low energies the spin is entirely collinear along z this means that more specifically they are eigenstates of L_z,

$$\langle n|L_z|n\rangle \equiv \lambda_n(\vec{k}). \tag{9}$$

As the OAM texture arises from the changing orbital character of the energy eigenstates and not any k-space variation in the OAM operator itself it is clear that

$$\langle n|\vec{\nabla}_{\vec{k}} L_z|n\rangle = 0. \tag{10}$$

Combining eq. (9) and eq. (10), and taking the $\vec{k}$ dependence of λ_n to be implicit,

$$\begin{aligned}
\partial_{k_i}\lambda_n &= \int \left[\partial_{k_i}(n^*) L_z n + n^* \partial_{k_i}(L_z) n + n^* L_z \partial_{k_i} n\right] d\vec{r}^3 \\
&= \int \left[n^* L_z \partial_{k_i} n - (\partial_{k_i} n)^* L_z n\right] d\vec{r}^3 \\
&= \langle n|L_z|\partial_{k_i} n\rangle - \langle\partial_{k_i} n|L_z|n\rangle \\
&= \lambda_n(\langle n|\partial_{k_i} n\rangle - \langle\partial_{k_i} n|n\rangle),
\end{aligned} \tag{11}$$

where we have used the anti-Hermitian property of ∂_{k_i}. From this we write,

$$\begin{aligned}
\partial_{k_j}\left(\frac{\partial_{k_i}\lambda_n}{\lambda_n}\right) &= \langle\partial_{k_i} n|\partial_{k_j} n\rangle + \langle\partial_{k_j} n|\partial_{k_i} n\rangle - \langle\partial_{k_j}\partial_{k_i} n|n\rangle - \langle n|\partial_{k_j}\partial_{k_i} n\rangle \\
&= 4\langle\partial_{k_i} n|\partial_{k_j} n\rangle,
\end{aligned} \tag{12}$$

Hence,

$$\left|\vec{\Omega}_n(\vec{k})\right|^2 \propto \sum_{i,j,p,q} \left(\partial_{k_j}\left(\frac{\partial_{k_i}\lambda_n}{\lambda_n}\right)\right)^2 - \partial_{k_p}\left(\frac{\partial_{k_p}\lambda_n}{\lambda_n}\right)\partial_{k_q}\left(\frac{\partial_{k_q}\lambda_n}{\lambda_n}\right). \tag{13}$$